Further Study on Effects of Hydrogen Addition on Laminar Flame Speeds of Fuel-Air Mixtures

Fujia Wu, Andrew P. Kelley, Delin Zhu and Chung K. Law

Department of Mechanical and Aerospace Engineering,
Princeton University, Princeton, NJ 08544

Laminar flame speeds of mixtures of ethane, ethylene, acetylene, and carbon monoxide with small amounts of hydrogen addition at both atmospheric and elevated pressures were experimentally and computationally determined. It was found that the approximate linear correlation identified previously between the laminar flame speeds and an appropriate definition of the amount of hydrogen addition for methane, propane and n-butane at atmospheric pressure also largely applies to ethylene, ethane and acetylene, at both normal and elevated pressures, with the dependence for rich ethane-air mixtures and lean acetylene-air exhibiting minor deviations from linearity. The linear correlation, however, does not hold for carbon monoxide, at all pressures, due to the strong catalytic effect of hydrogen on carbon monoxide oxidation. A mechanistic analysis shows that both the Arrhenius and diffusive contribution to laminar flame speeds are near-linear functions of hydrogen addition, which explains this approximate linear correlation.

1. Introduction

The strong reactivity of hydrogen makes it an attractive additive to enhance flame propagation speeds and extend the flammability limits of fuel-air mixtures, and as such offers rich potential to promote combustion efficiency and reduce pollutant emissions. The fundamental combustion parameter that compactly characterizes and quantifies the effects of hydrogen addition is the laminar flame speed, which embodies information about the exothermicity, reactivity and diffusivity of the resulting mixture.

In 1959, Scholte and Vaags [1,2] measured the flame speeds of hydrogen-methane and hydrogen-carbon monoxide mixtures with a tube burner. More recently [3-31], experimental work on effects of hydrogen addition has seen conducted using the expanding spherical flame method [3,4,9-11,14-24,26,28,31], the counterflow stagnation flame method [5,6,8,27,29], the flat-burner flame method [7,12,13,25] and the Bunsen flame method [29,30]. These studies have covered hydrogen mixtures with methane [3-6,8-10,12-16,20-22,25], ethylene [9], acetylene [4], propane [3,4,6,9,17,18], n-butane [7,24], iso-octane [16,23], carbon monoxide [2,26-31] and natural gas [11,19]. Most of these studies [1-5,8-23,25-31] have employed the hydrogen mole fraction in the fuel mixture to characterize the amount of hydrogen addition. The results for hydrocarbon-air mixtures showed a weak dependence on hydrogen addition up to about 50% hydrogen mole fraction, and a rapid increase thereafter. For carbon monoxide, however, hydrogen addition increases the flame speed rapidly with small hydrogen mole fraction in a catalytic manner.

Yu *et al*. [6] used the symmetric counterflow flame to measure the laminar flame speeds of methane-air and propane-air mixtures with hydrogen addition, and characterized the amount of addition with a parameter R_H, which will be defined later. The results showed that regardless of whether the mixture was lean or rich, the increase in the flame speed can be approximately linearly correlated with R_H. This simple correlation has generated considerable interest with substantial follow-on investigations. In particular, Sher and Ozdor [7] and Tang *et al*. [24] used the flat-burner flame method and the expanding spherical flame method, respectively, to measure the laminar flame speeds of n-butane-air mixtures with hydrogen addition, and found that the linear correlation again holds approximately. Additionally, Tang *et al* .[24] noted that hydrogen addition influences the flame speed through increasing the flame temperature (kinetic effect), intensifying the reactivity (kinetic effect) and facilitating the diffusion (diffusion effect). Furthermore, their sensitivity-based analysis showed that the kinetic effect is the most important among the three effects, followed by the thermal effect, while the diffusion effect is minimal.

The primary motivation for the present investigation is the recognition that while the approximate linear correlation has been demonstrated for three fuels, namely methane [6], propane [6] and n-butane [7,24], they are all n-alkanes and as such have similar kinetic and thermal characteristics. Because of the strong kinetic and thermal effects associated with hydrogen addition, as demonstrated in [24], it behooves us to extend the investigation to fuels with distinctively different kinetic and thermal characteristics. We shall conduct our assessment along the following three directions.

First, we shall study the C_2-group of the paraffins, namely ethane, ethylene and acetylene, because they have distinctively different kinetic and thermal properties among themselves. Furthermore, since they have similar diffusivities, potential differences in the diffusion effect are suppressed. Second, we shall also use carbon monoxide as a target fuel because hydrogen is known to have a strong catalytic effect on the oxidation of carbon monoxide and as such its use would provide a critical assessment on the potential deviation from linearity due to strong kinetic coupling. Third, we shall further manipulate the kinetic effect by performing experiments under elevated pressures, recognizing the strong kinetic influence on the progress of reactions through pressure variations.

Results from these three series of assessments will be presented in the following, after specifications of the experimental and computational aspects of the investigation.

2. Methodology

2.1 Experimental setup

The laminar flame speed was determined using expanding spherical flames, employing the dual-chamber design of Tse *et al*. [32]. This apparatus has been used to generate extensive amounts of data on the laminar flame speeds of a variety of fuels in recent years. Details of the design and operational procedure are given in Ref. [32]. Briefly, it consists of a small inner chamber surrounded by a substantially larger outer chamber. The inner chamber is filled with the test mixture while the outer chamber is filled with a mixture of inert gases and matches the density and pressure of the inner chamber. The combustible mixture in the inner chamber is spark ignited resulting in an expanding spherical flame. At the moment of spark ignition a series of holes are aligned to connect the inner and outer chambers such that flame propagation is

automatically quenched as the flame reaches the interface of the inner and outer chambers. This dual-chamber design also ensures that flame propagation takes place at constant chamber pressure and upstream temperature due to the large volume of inert gas in the outer chamber. The maximum pressure rise has been measured to be less than 3% for the entire chamber [32]. The time-resolved schlieren flame images are recorded using a high-speed digital camera and the flame radius can be determined as a function of time by tracking the flame front image.

Standard air was used as the oxidizer for measurements at atmospheric pressure. At elevated pressures we used oxygen-helium mixture, because helium has a higher thermal conductivity than nitrogen and thus can increase the mixture's Lewis number and further suppress cellular instabilities [33,34]. All hydrocarbon fuels used have a minimum purity of 99.5% while hydrogen has a purity of 99.99% and carbon monoxide has a purity of 99.99% with total moisture, hydrogen and hydrocarbon concentrations being less than 10 ppm. The air or oxygen-inert mixtures used are synthetic mixtures of pure oxygen and pure inert (nitrogen or helium), both of which have a minimum purity of 99.99%; however, the oxygen-inert ratio in these mixtures has a relative uncertainty of approximately $\pm 2\%$. The experimental uncertainty in the equivalence ratio is approximately $\pm 2\%$ and the hydrogen addition parameter, R_H, to be defined, has an absolute uncertainty of approximately ± 0.005.

2.2 Data analysis

The experimental data from expanding spherical flames was used to extrapolate the laminar flame speed using a nonlinear extrapolation equation recently derived by Kelley *et al.* [35],

$$S_b^0 = \frac{dr_f}{dt}(1 + \frac{2L_b}{r_f} + \frac{4L_b^2}{r_f^2} + \frac{16L_b^3}{3r_f^3})$$ (1)

where S_b is the adiabatic unstretched burned gas speed relative to the flame, S_f the flame radius, L_b the Markstein length and t the time. This equation is derived from an asymptotic analysis based on large activation energy for premixed flame allowing general Lewis numbers. Equation (1) could be integrated, yielding

$$S_b^0 t + C = r_f + 2L_b \ln r_f - \frac{4L_b^2}{r_f} - \frac{8L_b^3}{3r_f^2}$$ (2)

based on which a least-square fitting with experimental data r_f and t can be performed to determine S_b^0 and L_b. The laminar flame speed, S_u^0, which is defined to be the unstretched unburned gas speed relative to flame, can then be calculated from the continuity relation,

$$\rho_u^0 S_u^0 = \rho_b^0 S_b^0$$ (3)

where ρ_u^0 and ρ_b^0 are respectively the unburned and burned gas densities of the freely propagating steady planar adiabatic premixed flame, which can be calculated.

For flame speed measurement using expanding spherical flames, data in certain radius range has to be chosen for extrapolation, *i.e.*, the small radii data should be removed to eliminate the influence of ignition and the large radii data should be removed to eliminate the hydrodynamic influence of the chamber wall. In the present study, we used the data in the radius range between 0.7 cm and 1.5 cm. Based on repeated measurements and the sensitivity of selection of the data

range for extrapolation, all reported laminar flame speeds in this paper have an absolute uncertainty of ± 1.5 cm/s and relative uncertainty of $\pm 4\%$ approximately.

2.3 Composition parameters

In a fuel-air mixture with hydrogen addition there are two fuels and one oxidizer in the system, therefore we need two parameters to represent its composition, respectively designating the fuel-oxidizer ratio and the amount of hydrogen addition. The parameters used by most previous researchers are the overall equivalence ratio, ϕ, and the mole fraction of hydrogen in the fuel mixture, α, respectively defined as

$$\phi = \frac{C_F / C_A}{(C_F / C_A)_{st}} + \frac{C_H / C_A}{(C_H / C_A)_{st}} \tag{4}$$

$$\alpha = \frac{C_H}{C_H + C_F} \tag{5}$$

where C_F, C_H and C_A are the mole concentrations of the dominant fuel, hydrogen and air respectively; and the subscript *st* designates the value at the stoichiometric condition. For instance, for hydrogen in air the values of $(C_H / C_A)_{st}$ is 0.42 and for ethylene the value of $(C_F / C_A)_{st}$ is 0.07. These definitions imply that the oxidizer is equally available to both the dominant fuel and hydrogen; in other words, they have the same priority to react with oxygen. However, hydrogen as a fuel is special from any other fuel in two aspects: 1) it is highly reactive; 2) it is highly diffusive. Therefore it is reasonable to assume that hydrogen has a stronger tendency to react with oxygen, especially considering that in most studies the amount of hydrogen addition is small in terms of the oxygen consumption.

Following this concept, the following composition parameters were defined in Ref. [6]:

$$\phi_F = \frac{C_F / [C_A - C_H / (C_H / C_A)_{st}]}{(C_F / C_A)_{st}} \tag{6}$$

$$R_H = \frac{C_H + C_H / (C_H / C_A)_{st}}{C_F + [C_A - C_H / (C_H / C_A)_{st}]} \tag{7}$$

These definitions imply that there is always enough oxygen to facilitate the complete oxidation of hydrogen. If this is the case, then the remaining oxygen would react with the abundant fuel. Therefore, ϕ_F of Eq. (6) represents an effective equivalence ratio of the abundant fuel. Base on this, Equation (7) defines a parameter R_H representing the amount of hydrogen addition, *i.e.*, the ratio of the total mole concentration of the hydrogen-air mixture to the total mole concentration of the abundant fuel-air mixture. When $R_H = 0$, there is no hydrogen present; when R_H approaches ∞, the mixture approximates a stoichiometric hydrogen-air mixture. For large amount of hydrogen addition ϕ_F and R_H should not be used because in such cases complete oxidation of hydrogen cannot be justified.

2.4 Computational specification

Laminar flame speeds were calculated using the Chemkin Premix code. The solution was obtained allowing multi-component formulation of transport properties and thermal diffusion. The kinetic mechanism employed in the present study is USC Mech II [36], a high-temperature reaction model consisting of 111 species and 784 reactions. The mechanism was developed for prediction of $H_2/CO/C_1$-C_4 hydrocarbon combustion.

In order to provide meaningful interpretation of the results, some kinetic and transport parameters of the resulting mixtures were also calculated using USC Mech II. Recognizing the following theoretical relation on the laminar flame speed

$$S_u^0 \sim (\alpha Le)^{\frac{1}{2}} \exp(-T_a / 2T_{ad}) \tag{8}$$

where α is the thermal diffusivity, Le the Lewis number, T_a the overall activation temperature, and T_{ad} the adiabatic temperature. The relation is based on a global, one-step reaction for a premixed flame, with the effects of kinetics and diffusion embedded by allowing the global parameters to vary with the mixture parameters, defined next.

In the present study, we follow the same methodology in Ref. [24] to evaluate the above parameters. Briefly, the global activation temperature T_a is extracted through the relation [33]

$$T_a = -2 \frac{d \ln(f)}{d(1/T_{ad})} \tag{9}$$

where f is the laminar burning flux. The small perturbation in flame temperature in Equation (9) is achieved by replacing small amount of nitrogen with argon in the mixture. Thermal diffusivity α and other transport coefficients are calculated using the Chemkin Transport program and evaluated at unburned gas temperature for simplicity. The effective Lewis number of the entire mixture is calculated from the following equations derived in [37,38]

$$Le_{HF} = 1 + \frac{q_H(Le_H - 1) + q_F(Le_F - 1)}{q_H + q_F} \tag{10}$$

$$Le_{eff} = \begin{cases} 1 + \dfrac{(Le_{HF} - 1) + [1 + Ze(\phi_F - 1)](Le_O - 1)}{2 + Ze(\phi_F - 1)}, & \text{for } \phi_F > 1 \\[3ex] 1 + \dfrac{[1 + Ze(\phi_F^{-1} - 1)](Le_{HF} - 1) + (Le_O - 1)}{2 + Ze(\phi_F^{-1} - 1)}, & \text{for } \phi_F < 1 \end{cases} \tag{11}$$

where Le_H, Le_F and Le_O are the Lewis numbers of hydrogen, fuel and oxygen; q_H and q_F are the nondimensional heat releases of the hydrogen and fuel in the mixture; and Ze is the Zel'dovich number.

Having determined the above parameters, the influence of hydrogen addition due to different effects can be evaluated. We notice in Equation (8) that the kinetic and thermal effects are lumped through the exponential factor $\exp(-T_a / 2T_{ad})$, therefore they can be treated together as a combined Arrhenius effect. Similarly, $(\alpha Le)^{1/2}$ represents the diffusion effect.

3. Results and discussion

3.1 Results on ethylene, ethane and acetylene

The measured and calculated laminar flame speeds of ethane-air, ethylene-air and acetylene-air mixtures with hydrogen addition at atmospheric pressure are shown in Figures 1-3. Three values of ϕ_F: 0.7, 1.0 and 1.6 were chosen for each fuel. All curves are plotted as a function of R_H. In addition, the laminar flame speed is correlated with R_H by a linear relation [6],

$$s_u^0(\phi_F, R_H) = s_u^0(\phi_F, 0) + k(\phi_F)R_H \qquad (12)$$

where $k(\phi_F)$ is a coefficient that represents the sensitivity of the laminar flame speed to hydrogen addition. The values of $k(\phi_F)$ for both calculated and measured curves are also noted in Figures 1-3.

In terms of agreement between calculation and experiment, it is seen that the measured and calculated flame speeds agree reasonably well for ethylene. However, for ethane the calculation mostly over predicts the flame speeds, and for acetylene it over predicts the lean and stoichiometric flame speeds and under predicts the rich one. In addition, the calculated values of $k(\phi_F)$ are also mostly lower than measured ones for all curves except the rich acetylene mixture. These disagreements simply indicate that the reaction mechanism is not sufficiently comprehensive in its description of the diverse range of the experiments conducted herein.
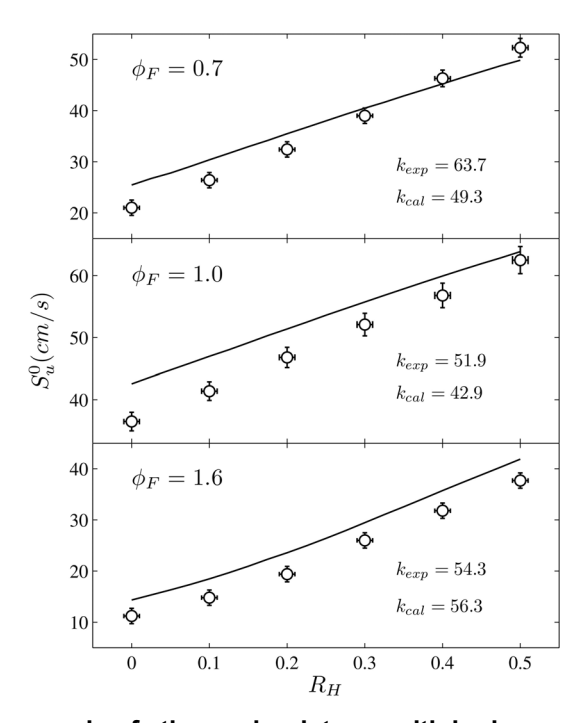

Figure 1: Laminar flame speeds of ethane-air mixtures with hydrogen addition at atmospheric pressure (initial temperature: 293K±2K; circles: measured results; solid lines: calculated results using USC Mech II)
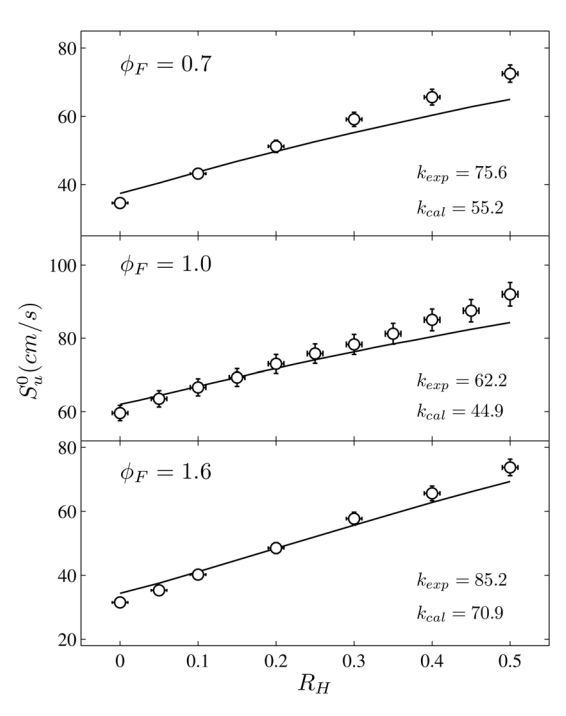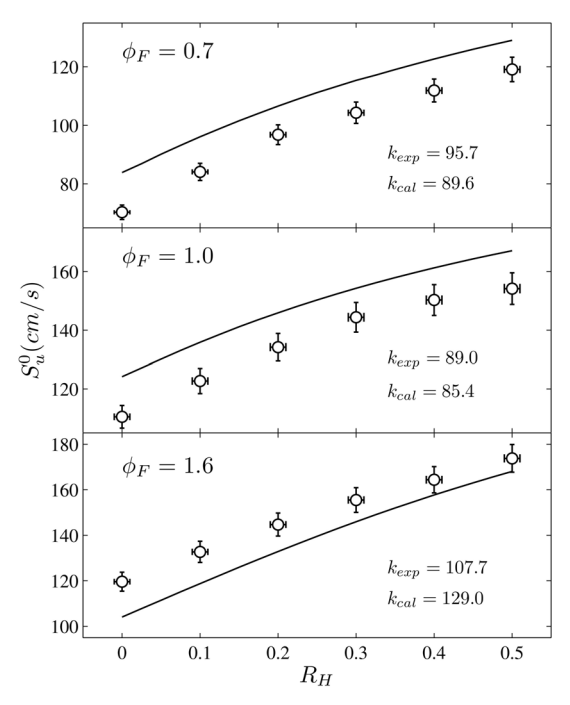
Figure 2: Laminar flame speeds of ethylene-air mixtures with hydrogen addition at atmospheric pressure (initial temperature: 293K±2K; circles: measured results; solid lines: calculated results using USC Mech II)

Figure 3: Laminar flame speeds of acetylene-air mixtures with hydrogen addition at atmospheric pressure (initial temperature: 293K±2K; circles: measured results; solid lines: calculated results using USC Mech II)

Figures 1-3 shows that the correlations between laminar flame speeds and R_H for all three fuels are approximately linear. This therefore corroborates the linear correlation previously observed for methane, propane and n-butane mixtures [6,7,24], even for the present fuels of distinctively different kinetic and thermal properties. Furthermore, the dependence of the flame speeds of ethylene-air mixtures on R_H exhibits the strongest linearity, while those of rich ethane-air mixtures and lean acetylene-air mixtures exhibit minor deviation from linearity. In particular, the flame speeds of rich ethane-air mixtures increase faster than the linear relationship for larger values of R_H, and conversely, the flame speeds of lean acetylene-air mixtures increase slower as R_H increases. However, despite the minor deviation the linear correlation between laminar flame speeds and R_H still approximately holds for all three fuels.

So far we have observed the linear correlation for various hydrocarbon fuels by both experiment and calculation; therefore it is fundamentally intriguing to seek the fundamental reasons. Through evaluation of the governing parameters of laminar flame propagation, we first calculated the values of the Arrhenius factor, diffusion factor and their product, normalized by their values at zero hydrogen addition to facilitate comparison, *i.e.*,

$$\text{Normalized Arrhenius factor} \;=\; \frac{\exp(-T_a/2T_{ad})}{\exp(-T_a^o/2T_{ad}^{\;o})} \tag{13}$$

$$\text{Normalized diffusion factor} \;=\; (\frac{\alpha Le}{\alpha^o Le^o})^{\frac{1}{2}} \tag{14}$$

$$\text{Normalized total factor} \;=\; (\frac{\alpha Le}{\alpha^o Le^o})^{\frac{1}{2}} \frac{\exp(-T_a/2T_{ad})}{\exp(-T_a^o/2T_{ad}^{\;o})} \tag{15}$$

where the superscript o indicates the respective values at $R_H = 0$.

The values of Equations (13-15) are plotted in Figures 4-6. It is seen that the normalized Arrhenius factor is mostly dominant over the normalized diffusion factor; this indicates the dependence of the Arrhenius factor on hydrogen addition should give the dominant dependence of laminar flame speeds. As shown in Figures 4-6, the Arrhenius factor is indeed a near-linear function of R_H for all three fuels, which is consistent with the approximate linear dependence of laminar flame speeds.

To further understand the dependence of the Arrhenius effect on hydrogen addition, we re-arrange the normalized Arrhenius factor as,

$$\frac{\exp(-T_a/2T_{ad})}{\exp(-T_a^o/2T_{ad}^{\;o})} = \exp[\frac{Ar^o}{2}(1-\frac{Ar}{Ar^o})] \tag{16}$$

where $Ar = T_a/T_{ad}$ is the Arrhenius number. The factor $(1 - Ar/Ar^o)$ in Equation (16) measures the relative modification of Ar by hydrogen addition from its original value Ar^o, *i.e.*, the percentage change in the mixture's kinetics by hydrogen. Its value is plotted in Figure 7 along with the normalized activation temperature, flame temperature and Arrhenius factor, for the ethylene-air mixture at $\phi_F = 1.6$ as an example. It is seen that the approximate linear dependence
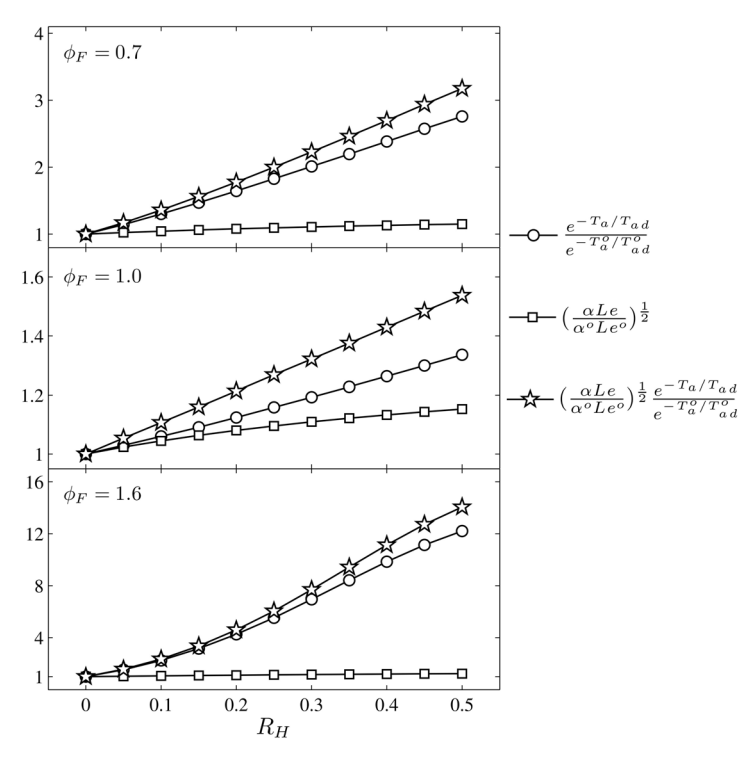
8

Figure 4: Normalized values of Arrhenius and diffusion factors by their values at zero hydrogen addition for ethane-air mixtures at atmospheric pressure (initial temperature: 293K)
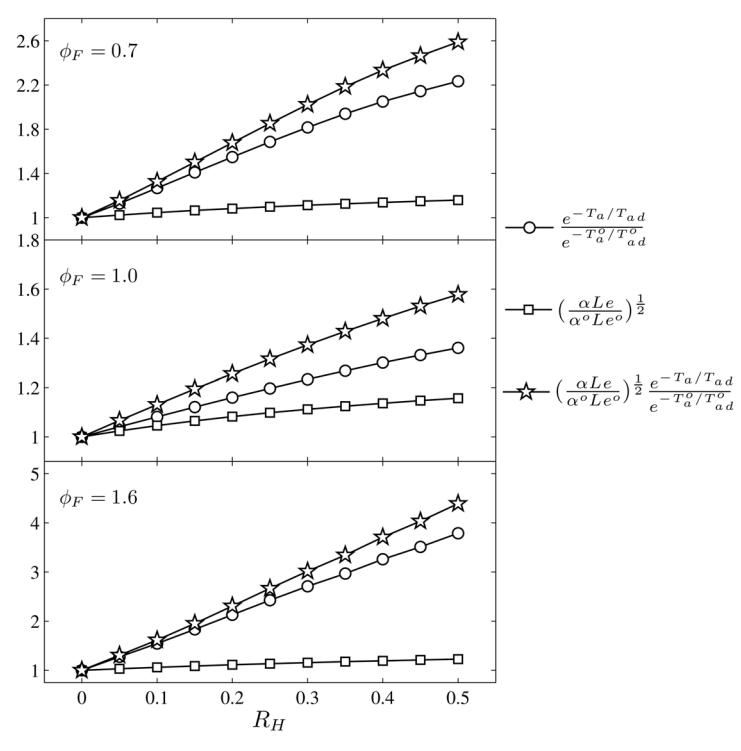

Figure 5: Normalized values of Arrhenius and diffusion factors by their values at zero hydrogen addition for ethylene-air mixtures at atmospheric pressure (initial temperature: 293K)
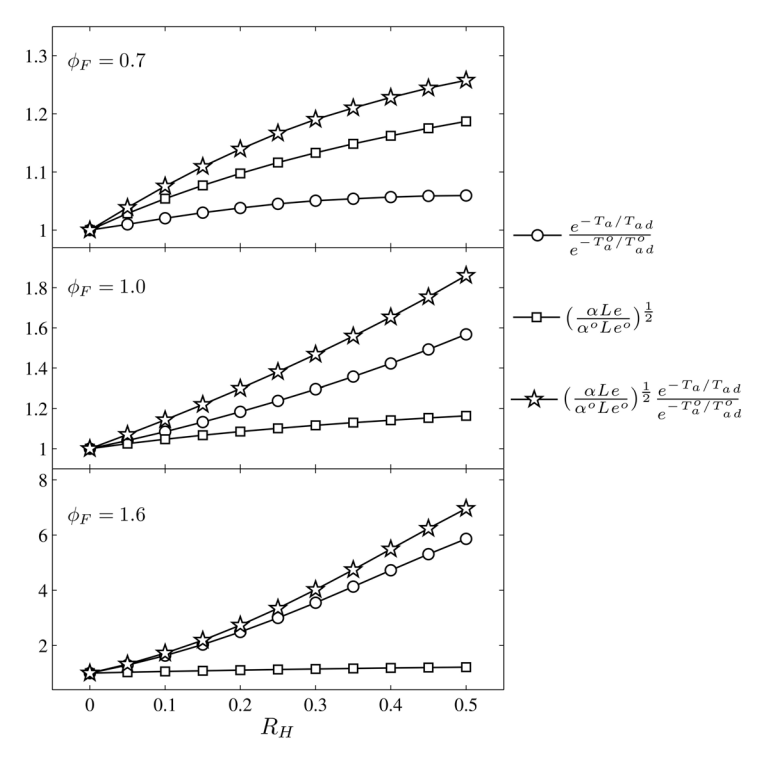
Figure 6: Normalized values of Arrhenius and diffusion factors by their values at zero hydrogen addition for acetylene-air mixtures at atmospheric pressure (initial temperature: 293K)
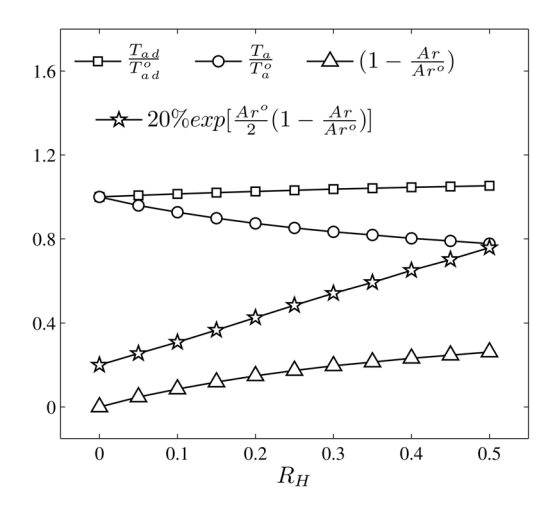

Figure 7: Normalized values of various factors that contribute to the Arrhenius factor for a rich ethylene-air mixture with hydrogen addition at atmospheric pressure (initial temperature: 293K; ϕ_F = 1.6)

of the Arrhenius factor on hydrogen addition is because the value of $(1 - Ar/Ar^o)$ varies with R_H in a logarithm-like curve, leading to a linear variation after exponentiation. We further notice that the changes in $(1 - Ar/Ar^o)$ are mainly due to the modification of the activation temperature rather than the flame temperature; in other words, kinetic effect is stronger than the

thermal effect. This logarithm-like dependence of the kinetic effect is reasonable because as more hydrogen is added its effect on the fuel oxidation becomes gradually saturated.

The secondary cause for the linear correlation is the dependence of the diffusion factor on hydrogen addition. It is seen from Figures 4-6 that the normalized diffusion factor is also a near-linear function of R_H, which then contributes to the dependence of the combined factor. This therefore further explains the observed linear dependence of laminar flame speeds on hydrogen addition. For instance, different from other cases the diffusion factor for the lean acetylene-air mixture is larger than the kinetic factor. This indicates that the flame speed is increased by hydrogen mainly through facilitated heat and mass diffusion. This is reasonable because acetylene is characterized by strong reactivity and high exothermicity, and as such hydrogen addition is not necessary an enhancement to its oxidation kinetics. However, despite the difference in the dominant effect, for this lean acetylene-air mixture the dependence of laminar flame speed on hydrogen addition is still approximately linear.
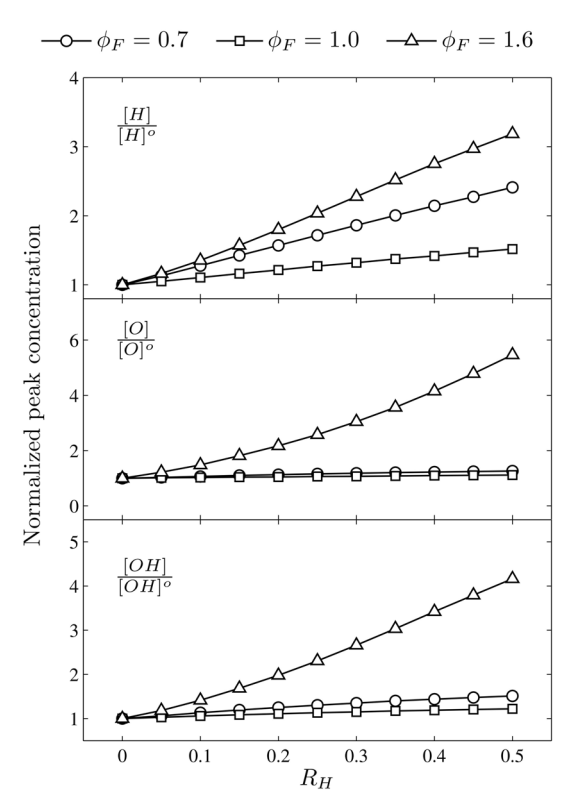

Figure 8: Peak H, O and OH concentrations normalized by their values at zero hydrogen addition in the 1-D planar flame of ethylene-air mixtures with hydrogen addition at atmospheric pressure (initial temperature: 293K; the superscript, o, indicates the values at zero hydrogen addition)

Another conclusion that can be drawn from Figures 1-3 is that the sensitivity coefficient $k(\phi_F)$ of laminar flame speeds to hydrogen addition seems always exhibits a minimum at $\phi_F = 1$, which agrees with previous result for n-butane in Ref. [24]. Such dependence indicates that the effect of hydrogen addition is stronger at off-stoichiometric, weak burning conditions than around stoichiometry where the burning is strong even without hydrogen addition. Figure 8 plots the peak H, O and OH radical concentrations in the standard 1-D planar flame as a function of

R_H for lean, stoichiometric and rich ethylene-air mixtures. The concentrations are again normalized by their respective values at $R_H = 0$. It is seen clearly that for the stoichiometric mixtures, the values of H, O and OH radicals due to hydrogen addition are always minimum, which is consistent in the dependence of the laminar flame speeds.

3.2 Results on carbon monoxide

The measured and calculated flame speeds of carbon monoxide-air mixtures with hydrogen addition at atmospheric pressure, for three values of ϕ_F: 0.7, 1.0 and 1.6 are shown in Figure 9. First, good agreement between calculation and experiment is seen for all three curves both in the values of laminar flame speeds and their dependence on hydrogen addition, hence demonstrating the satisfactory state of the oxidative mechanism of carbon monoxide. In addition, different from hydrocarbon-air mixtures the laminar flame speed of carbon monoxide-air mixture with hydrogen addition exhibits a highly nonlinear dependence on R_H: 1) The laminar flame speed of pure carbon monoxide-air mixture is very close to zero. In fact, in experiments it was not possible to initiate an expanding spherical flame with a pure carbon monoxide mixture. 2) The laminar flame speed increases rapidly as R_H increases from 0 to 0.1. 3) Further increasing R_H beyond 0.1 results in a nearly linear relationship.
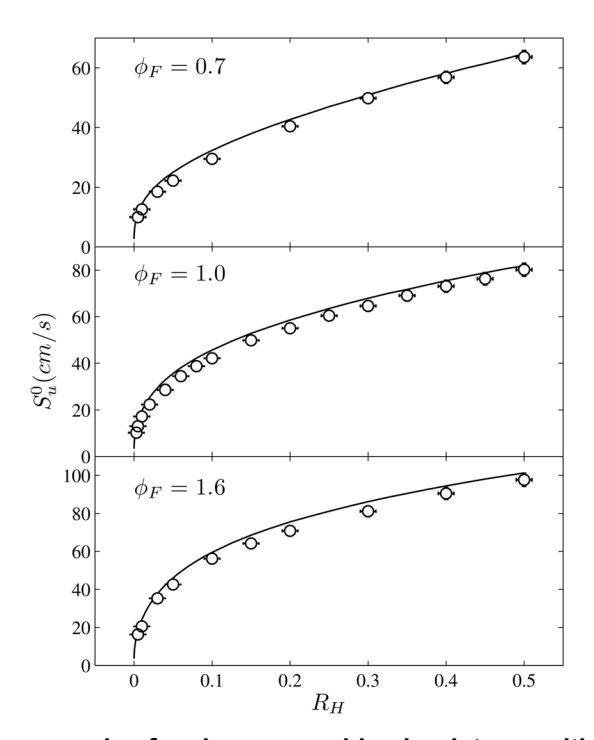

Figure 9: Laminar flame speeds of carbon monoxide-air mixtures with hydrogen addition at atmospheric pressure (initial temperature: 293K±2K; circles: measured results; solid lines: calculated results using USC Mech II)

The same analysis is performed for carbon monoxide by evaluating the governing parameters of flame propagation. The normalized Arrhenius and diffusion are plotted in Figure 10 with the case at $\phi_F = 1.0$ as an example. The normalized activation temperature and flame temperature as well as the values of $(1 - Ar / Ar^o)$ are plotted in Figure 11. As expected, we notice a dominant Arrhenius factor over the diffusion factor and the increase in Arrhenius factor is not due to

modification of the flame temperature but the activation temperature. The difference from hydrocarbons is that the kinetic effect of hydrogen on carbon monoxide oxidation is much stronger, especially for small values of R_H. This strong catalytic effect substantially reduces the activation temperature and consequently increases the Arrhenius factor, leading to a nonlinear dependence of the laminar flame speed R_H. However, for the values of R_H larger than 0.2 the modification of the activation temperature by hydrogen becomes much smaller, and the kinetic effect becomes moderate and is comparable with the diffusion effect, hence again leading to an approximate linear dependence of Arrhenius factor and thus the laminar flame speeds. This indicates the catalytic effect becomes saturated as more hydrogen is present in the mixture.
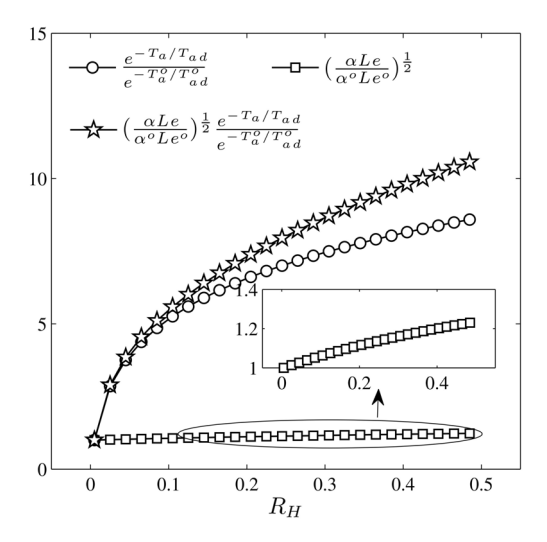

Figure 10: Normalized values of Arrhenius and diffusion factors in Equation (8) by their values at no hydrogen addition for a stoichiometric carbon monoxide-air mixture with hydrogen addition at atmospheric pressure (initial temperature: 293K)
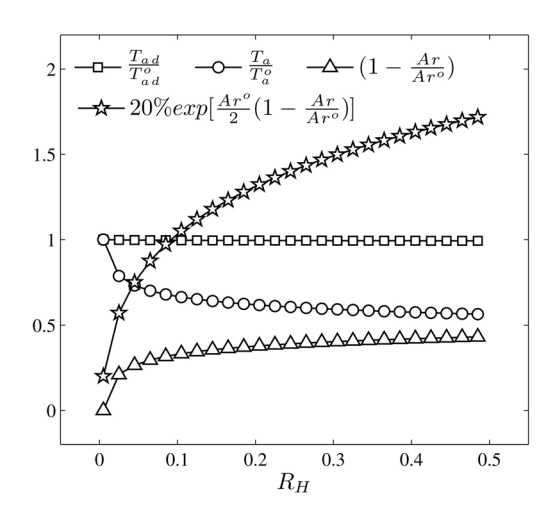

Figure 11: Normalized values of various factors that contribute to the Arrhenius factor for a stoichiometric carbon monoxide-air mixture with hydrogen addition at atmospheric pressure (initial temperature: 293K)

3.3 Results at elevated pressures

Experiments at elevated pressure were conducted for three cases: 1) an ethylene-air mixture at $\phi_F = 0.7$ and pressure of 5 atm; 2) a propane-oxygen-helium mixture at $\phi_F = 0.6$ and pressure of 20 atm with reduced oxygen concentration; 3) a carbon monoxide-oxygen-helium mixture at $\phi_F = 1.0$ and pressure of 20 atm.
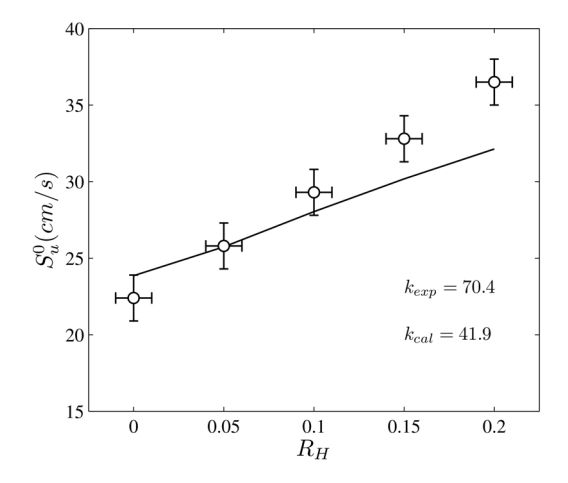

Figure 12: Laminar flame speeds of ethylene-air mixtures with hydrogen addition at ϕ_F = 0.7 at pressure = 5 atm (initial temperature: 293K±2K; circles: measured results; solid lines: calculated results with USC Mech II)
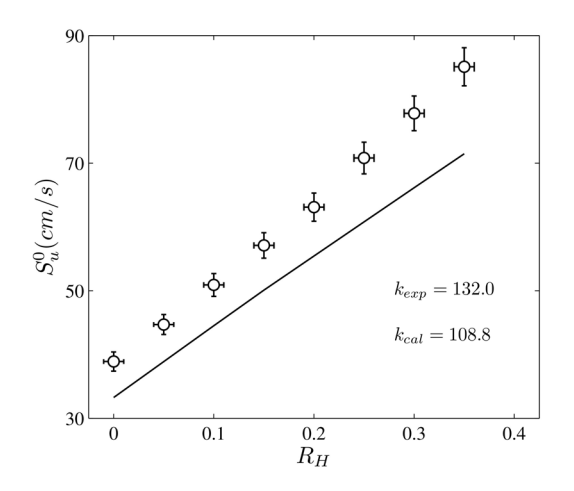

Figure 13: Laminar flame speeds of propane-oxygen-helium mixtures with hydrogen addition at ϕ_F = 0.6 at pressure = 20 atm (O2 Vol.%: He Vol.%: 12.5:87.5; initial temperature: 293K±2K; circles: measured results; solid lines: calculated results using USC Mech II)

Figure 12 shows the measured and calculated flame speeds of the lean ethylene-air mixture at 5 atm. It is seen that there are finite differences between experiment and calculation particularly in the values of the sensitivity coefficient k. Nevertheless both curves show approximate linear correlation between laminar flame speeds and R_H. Only results at R_H from 0 to 0.2 are shown because the flame speed measurement is only possible for small values of R_H, as further

increasing R_H causes cellular instabilities to develop because the presence of hydrogen reduces the effective Lewis number of the mixture and promotes the diffusion-thermal cellular instability [33,34]. This phenomenon does not appear at atmospheric pressure because the flame is thicker and can always stabilize an expanding spherical flame at lower pressures.

Figure 13 shows the measured and calculated flame speeds of the lean propane-air mixture at 20 atm. As pressure increases the flame becomes harder to stabilize because of the decrease in flame thickness. Therefore to further suppress cellular instabilities, at 20 atm, we used propane since its lean mixture has higher Lewis number and helium instead of nitrogen since helium can reduce the effective Lewis number of the mixture. It is seen from Figure 13 that the calculation largely under predicts the flame speeds and the sensitivity coefficient k for this case. However, the approximate linear correlation between laminar flame speeds and R_H still holds for both measured and calculated results even at the pressure of 20 atm. The linear correlation of hydrogen addition on laminar flame speeds for hydrocarbon-air mixtures is therefore extended to normal and elevated pressures.
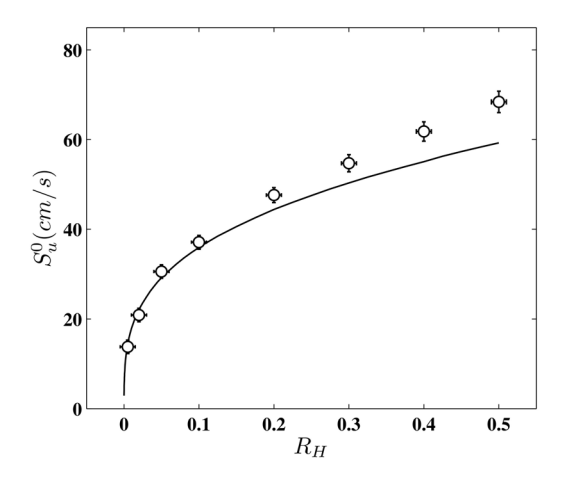

Figure 14: Laminar flame speeds of carbon monoxide-oxygen-helium mixture with hydrogen addition at ϕ_F = 1.0 at pressure = 20 atm (O2 Vol.%: He Vol.%: 12.5:87.5; initial temperature: 293K±2K; circles: measured results; solid lines: calculated results using USC Mech II)

Figure 14 shows the measured and calculated laminar flame speeds of the carbon monoxide-oxygen-helium mixture at $\phi_F = 1.0$ at the pressure of 20 atm. It is seen that while the calculation and experiment have good agreement for small hydrogen addition, it under predicts the flame speed at high hydrogen addition. The overall agreement between calculation and experiment is not as good as those at atmospheric pressure. In addition, different from hydrocarbon fuels the flame speed in Figure 14 shows a nonlinear dependence on R_H, which is in similar trend as the results at atmospheric pressure. This indicates that the influence of hydrogen addition on carbon monoxide oxidation is still characterized by the catalytic effect.

4. Concluding Remarks

The following conclusions can be made from the present study:

1) The approximate linear correlation between laminar flame speed and hydrogen addition was experimentally and computationally demonstrated for ethylene, acetylene and ethane, with the sensitivity coefficient, *k,* exhibiting a minimum around stoichiometry.

2) A mechanistic analysis based on evaluation of the governing flame parameters shows that both the Arrhenius and diffusive contributions to laminar flame speeds are near-linear functions of hydrogen addition, which explains the approximate linear correlation identified.

3) Linear correlation between laminar flame speeds and hydrogen addition was also experimentally and computationally demonstrated to approximately apply for ethylene and propane at normal and elevated pressures;

4) Different from hydrocarbon fuels, the increase in laminar flame speed of carbon monoxide exhibits a highly nonlinear dependence with hydrogen addition due to the strong catalytic effect on its oxidation.

Acknowledgments

References

[1] T. G. Scholte, P. B. Vaags, Combustion and Flame 3 (1959) 511-524.
[2] T. G. Scholte, P. B. Vaags, Combustion and Flame 3 (1959) 503-510.
[3] S. Refael, E. Sher, Combustion and Flame 78 (1989) 326-338.
[4] B. E. Milton, J. C. Keck, Combustion and Flame 58 (1984) 13-22.
[5] Y. Liu, B. Lenze, W. Leuckel, Progress in Astronautics and Aeronautics 131 (1991) 259-274.
[6] G. Yu, C. K. Law, C. K. Wu, Combustion and Flame 63 (1986) 339-347.
[7] E. Sher, N. Ozdor, Combustion and Flame 89 (1992) 214-220.
[8] J. Y. Ren, W. Qin, F. N. Egolfopoulos, T. T. Tsotsis, Combustion and Flame 124 (2001) 717-720.
[9] C. K. Law, O. C. Kwon, International Journal of Hydrogen Energy 29 (2004) 867-879.
[10] F. Halter, C. Chauveau, I. Gokalp, International Journal of Hydrogen Energy 32 (2007) 2585-2592.
[11] Z. Huang, Y. Zhang, K. Zeng, B. Liu, Q. Wang, D. Jiang, Combustion and Flame 146 (2006) 302-311.
[12] F. H. V. Coppens, J. de Ruyck, A. A. Konnov, Experimental Thermal and Fluid Science 31 (2007) 437-444.
[13] F.H.V. Coppens, J. de Ruyck, A. A. Konnov, Combustion and Flame 149 (2007) 409-417.
[14] M. Ilbas, A. Crayford, I. Yilmaz, P. Bowen, N. Syred, International Journal of Hydrogen Energy 31 (2006) 1768-1779.
[15] F. Halter, C. Chauveau, N. Djebaili-Chaumeix, I. Gokalp, Proceedings of the Combustion Institute 30 (2005) 201-208.
[16] C. Mandilas, M. P. Ormsby, C. G. W. Sheppard, R. Woolley, Proceedings of the Combustion Institute 31 (2007) 1443-1450.
[17] C. Tang, Z. Huang, C. Jin, J. He, J. Wang, X. Wang, H. Miao, International Journal of Hydrogen Energy 33 (2008) 4906-4914.
[18] C. Tang, J. He, Z. Huang, C. Jin, J. Wang, X. Wang, H. Miao, International Journal of Hydrogen Energy 33 (2008) 7274-7285.
[19] H. Miao, Q. Jiao, Z. Huang, D. Jiang, International Journal of Hydrogen Energy 34 (2009) 507-518.
[20] E. Hu, Z. Huang, J. He, H. Miao, International Journal of Hydrogen Energy 34 (2009) 6951-6960.
[21] E. Hu, Z. Huang, J. He, C. Jin, J. Zheng, International Journal of Hydrogen Energy 34 (2009) 4876-4888.
[22] T. Tahtouh, F. Halter, E. Samson, C. Mounaïm-Rousselle, International Journal of Hydrogen Energy 34 (2009) 8329-8338.

[23]   T. Tahtouh, F. Halter, C. Mounaïm-Rousselle, International Journal of Hydrogen Energy 36 (2010) 985-991.

[24]   C. Tang, Z. Huang, C. K. Law, Proceedings of the Combustion Institute 33 (2011) 921-928.

[25]   R. T. E. Hermanns, A. A. Konnov, R. J. M. Bastiaans, L. P. H. de Goey, K. Lucka, H. Köhne, Fuel 89 (2010) 114-121.

[26]   I. C. Mclean, D. B. Smith, S. C. Taylor, Twenty-fifth International Symposium on Combustion (1994) 749-757.

[27]   C. M. Vagelopoulos, F. N. Egolfopoulos, Twenty-fifth International Symposium on Combustion (1994) 1317-1323.

[28]   H. Sun, S. I. Yang, G. Jomaas, C. K. Law, Proceedings of the Combustion Institute 31 (2007) 439-446.

[29]   J. Natarajan, T. Lieuwen, J. Seitzman, Combustion and Flame 151 (2007) 104-119.

[30]   C. Dong, Q. Zhou, Q. Zhao, Y. Zhang, T. Xu, S. Hui, Fuel 88 (2009) 1858-1863.

[31]   M. I. Hassan, K. T. Aung, G. M. Faeth, Journal of Propulsion and Power 13 (1997) 239-245.

[32]   S. D. Tse, D. Zhu, C. K. Law, Review of Scientific Instruments 75 (2004) 233-239.

[33]   C. K. Law, Combustion Physics, Cambridge University Press, 2006.

[34]   G. Jomaas, C. K. Law, J. K. Bechtold, Journal of Fluid Mechanics 583 (2007) 1-26.

[35]   A. P. Kelley, J. K. Bechtold, C. K. Law, 7th U.S. National Technical Meeting of the Combustion Institute, 2011.

[36]   H. Wang, X. You, V. J. Ameya, S. G. Davis, A. Laskin, F. Egolfopoulos, C.K. Law, USC Mech Version II, 2007.

[37]   C. K. Law, G. Jomaas, J. K. Bechtold, Proceedings of the Combustion Institute 30 (2005) 159-167.

[38]   J. K. Bechtold, M. Matalon, Combustion and Flame 127 (2001) 1906 -1913.